Astron. Astrophys. 330, 1120–1126 (1998)

ASTRONOMY AND ASTROPHYSICS

# Line profiles of H-like ions of C, N, and O in stellar plasmas

**J.-F. Gonzalez**[1,⋆], **C. Stehlé**[2], **M.-C. Artru**[1], **and G. Massacrier**[1]

[1] Centre de Recherche Astronomique de Lyon (CNRS-UMR 5574), Ecole Normale Supérieure de Lyon, 46 allée d'Italie, F-69364 Lyon Cédex 07, France

[2] Observatoire de Meudon, Département d'Astrophysique Relativiste et Cosmologie (CNRS-UPR 176), 5 place Jules Janssen, F-92165 Meudon Principal Cedex, France

Received 1 September 1997 / Accepted 29 September 1997

**Abstract.** Theoretical Stark profiles of Balmer and Lyman series of H-like ions of carbon, nitrogen, and oxygen are presented for a range of plasma conditions where these ions are dominant within their species. A convenient parametric formula is derived to fit the theoretical profiles, depending only on electronic density and the principal quantum number of the upper level of the transition. This analytic expression makes it easy to introduce these new profiles in many astrophysical applications.

The effect of including these profiles in the calculation of radiative acceleration ($g_{\rm rad}$) following the method developed in an earlier paper is presented. The contributions of bound-bound (b-b) transitions of H-like ions to $g_{\rm rad}$ is found to be smaller than previously computed, giving more importance to bound-free (b-f) and free-free (f-f) contributions.

**Key words:** atomic processes – diffusion – line: profiles – radiative transfer – stars: atmospheres

## 1. Introduction

The hydrogen-like ions, having one electron bound to a nucleus of charge $Z$, are affected by the linear Stark effect. Their lines are strongly broadened by interaction with charged particles of a surrounding plasma, as for example in stellar atmospheres and envelopes.

The tables of Vidal et al. (1973) provide line profiles in various plasma conditions for hydrogen lines of the Balmer and Lyman series. New theoretical calculations have been published by Stehlé (1994a). Recent results are also available for helium ($He^{+}$) by Schöning & Butler (1989) and Schöning (1994), and by Stehlé (1994b).

For others ions ($Z > 2$) a scaling of hydrogen profiles is generally done as a first estimate. However the range of plasma conditions should be extended for H-like ions and systematic detailed calculations are necessary to take correctly into account the effects of ion dynamics, which depend on $Z$. New theoretical results are provided by Stehlé (1996) who has given analytical profiles with tabulated parameters for a large number of $n \to n'$ transitions of any H-like ions.

**Table 1.** Plasma conditions used for the theoretical calculations.

| | Case 1 | Case 2 | Case 3 | Case 4 |
|---|---|---|---|---|
| $T$ (K) | $4.1 \times 10^5$ | $6.3 \times 10^5$ | $1.0 \times 10^6$ | $1.6 \times 10^6$ |
| $N_e$ (cm$^{-3}$) | $6.7 \times 10^{19}$ | $3.3 \times 10^{20}$ | $1.8 \times 10^{21}$ | $7.3 \times 10^{21}$ |

The purpose of this paper is to introduce the new theoretical results in a stellar application. Our example is the calculation of radiative accelerations on the abundant elements C, N and O in a wide range of plasma conditions, including those of stellar envelopes of A to F-type stars, according to the method developped by Gonzalez et al. (1995b; 1995a, hereafter GLAM and GAM).

When the concentration of a given species increases, its absorption efficiency saturates progressively and, simultaneously its contribution to the average radiative force decreases. This saturation effect is expected to be important for the ions of C, N and O, which are efficient absorbers. Line broadening is an important parameter to calculate their contribution to the radiative accelerations in the deep layers of stellar envelopes (temperature ranging from $10^5$ to $10^7$ K).

A parametrized formula is first elaborated to fit the theoretical line profiles of the ions $C^{5+}$, $N^{6+}$ and $O^{7+}$. It is the easiest way to allow a repetitive computation of many line profiles, a large number of times, with different plasma conditions: first for iteration on stellar depth, and secondly when considering inhomogeneous or time varying chemical mixtures.

Then the broadening of the lines of the H-like ions $C^{5+}$, $N^{6+}$ and $O^{7+}$ will be compared with previous results, namely those using rough approximations for the Stark profiles. Our parametrized profiles are then convoluted to a Doppler profile for a direct use in the computation of the radiative acceleration.

*Send offprint requests to*: M.-C. Artru

⋆ *Present address:* European Southern Observatory, Casilla 19001, Santiago 19, Chile

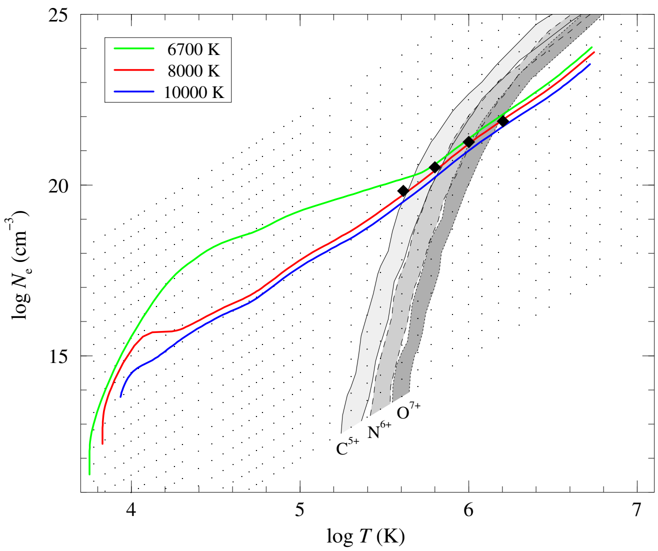


**Fig. 1.** Plasma conditions of the theoretical line profile calculations (diamonds). The shaded areas show the regions where the H-like ions of C, N, and O represent more than 50% of their species. The curves are models of stellar envelopes of $T_{\rm eff}$ = 6 700, 8 000, and 10 000 K. The grid points used in the calculation of GLAM are indicated by the dots.

## 2. Theoretical Stark profiles

The plasma conditions were chosen in view of our stellar application. Three standard models of stellar envelopes are displayed in Fig. 1. It also shows the range of temperature $T$ and electronic density $N_{\rm e}$ where the elements C, N and O are mainly in the hydrogen-like ionization stage is shown. We have calculated, for solar chemical composition, the detailed Stark profiles in four plasma conditions, located in this figure and given in Table 1. Hydrogen and helium are fully ionized. We computed line profiles for transitions in $C^{5+}$, $N^{6+}$ and $O^{7+}$ between levels of principal quantum number $n$ = 1 (Lyman series), $n$ = 2 (Balmer series) and a maximum value $n'$ = 14 for the upper level.

Line shapes are calculated on the basis of Model Microfield Method (Brissaud & Frisch 1971) with the dipolar contribution for the electrostatic interaction between the perturbers (ions and free electrons) and the radiating ion. Spontaneous decay is included in the calculations. The ionic contribution dominates the line centers whereas the electronic one dominates the wings.

The electronic contribution to the line shape is included through a damping operator $\gamma_{\rm e}(\omega)$, where $\omega = 2\pi\nu$ is the angular frequency, together with the radiative damping $\gamma_{\rm R}$. The ionic contribution is included in the same way as explained in Stehlé (1994b), allowing for the total damping operator $\gamma_{\rm e}(\omega) + \gamma_{\rm R}$ and for the exact plasma composition. The ionic field distribution function is estimated with the help of the Baranger & Mozer (1959, 1960) theory, which is justified for the present low correlated plasma conditions (Demura et al. 1995). This quantity depends on the charge of the perturbing ions which are mostly protons. We checked that we can assume that all perturbing ions have a charge equal to unity. The electronic damping operator $\gamma_{\rm e}(\omega)$ is obtained by a spline interpolation between the two known near-impact and static limits, in the line centers and wings respectively. The expressions for these limits are given in Eqs. (17)–(29) of Stehlé (1996) for the line centers, and (32)–(43) for the far wings. The near-impact limit is justified for detunings $\Delta\omega$ satisfying

$$\Delta\omega < \frac{< v_{\rm e} >}{\max(b_{\rm c}, a(kT))}, \tag{1}$$

where

$$< v_{\rm e} > = \sqrt{\frac{2kT}{m_{\rm e}}} \tag{2}$$

is the thermal electron velocity, $b_{\rm c}$ is the strong collision cutoff impact parameter defined in Eqs. (19) and (20) of Stehlé (1996) and

$$a(kT) = \frac{(Z-1)\,e^2}{kT} \tag{3}$$

is a measure of the range of the Coulombic interaction between the free electrons and the radiating H-like ion. The static limit is reached at large detunings, when

$$\Delta\omega > \frac{1}{t_{\rm s}}, \tag{4}$$

where the typical interaction time $t_{\rm s}$ is the ratio $r_{\rm s}/v_{\rm s}$ with

$$\begin{cases} r_{\rm s}^2 = \dfrac{3}{2}\dfrac{(n'^2 - n^2)\,e^2 a_0}{Z\hbar\Delta\omega} \\ \dfrac{1}{2}mv_{\rm s}^2 = kT + \dfrac{(Z-1)\,e^2}{r_{\rm s}} \end{cases} \tag{5}$$

(Greene & Cooper 1975). As in the case of hydrogen (Stehlé 1994a) we included the electronic contribution either with anisotropic electronic broadening for the lowest transitions ($n' \leq 7$) or with isotropic electronic broadening for the others ($n' > 7$). Balmer lines with $n' \geq 11$ were calculated with no lower state contribution. Taking into account our approximations we estimate that the pure Stark line shapes are correct within less than 20%. This accuracy is sufficient for most stellar applications.

Fine-structure effects modify the shapes of the lowest lines in Lyman and Balmer series ($n' \leq 4$). The corresponding line shapes have been calculated with the energy levels and dipolar strengths taken from the SUPERSTRUCTURE package (Eissner et al. 1974). Fig. 2 gives an example for lines $1 \rightarrow 2$ and $1 \rightarrow 4$ of $C^{5+}$ for case 1. The influence of fine structure for the Lyman lines, and a fortiori for the Balmer lines, on radiative diffusion is not significant in the present conditions, we thus neglect it in this paper. The proposed parametrization is therefore based on theoretical profiles computed without fine structure.

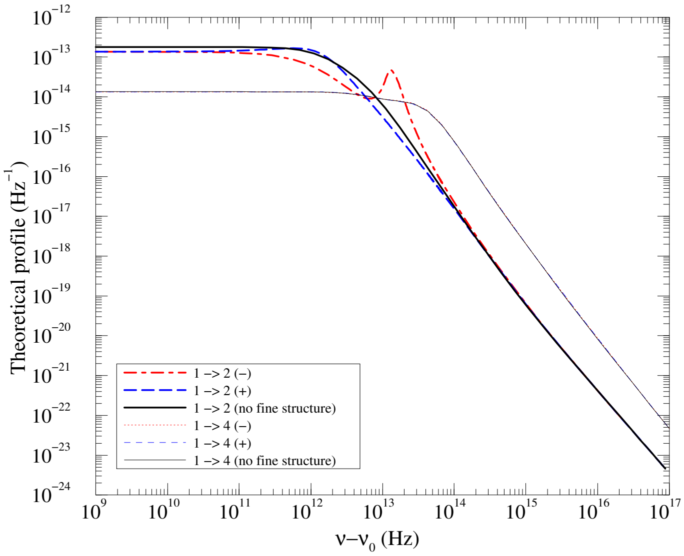


**Fig. 2.** Effect of the fine structure on the profiles of transitions $1 \longrightarrow 2$ and $1 \longrightarrow 4$ of $C^{5+}$ in case 1. The frequency $\nu_0$ refers to the unperturbed $1s_{\frac{1}{2}} \longrightarrow n' p_{\frac{3}{2}}$ transition. The labels − and + denote respectively the red and blue wings of the lines.

## 3. Parametrization of the profiles

We propose a simple parametric expression of the line profiles to fit the theoretical results presented in Sect. 2. The purpose is to compute easily the line profiles for every transition $n \longrightarrow n'$ of H-like ions (of nuclear charge $Z$) in a large domain of plasmas conditions (temperature $T$, electronic density $N_e$), achieving a compromise between a reasonable accuracy and a straightforward usefulness.

Our approach is a generalization of the parametrization proposed by Clausset et al. (1994) for the hydrogen lines of the Lyman and Balmer series. This new formulation makes the formulae much simpler. It is applied here to one-electron ions of carbon, nitrogen and oxygen.

The present parametrization concerns only the Stark profile and does not include the thermal Doppler effect. Therefore, convolution by a gaussian profile must be done afterwards (see Sect. 5). This choice allows a more regular behaviour of the parameters introduced in the analytic formula.

The Stark profile of the line $n \longrightarrow n'$ of central frequency $\nu_0$ for a one-electron ion (of nuclear charge $Z$ = 6, 7 or 8) perturbed by protons is approximated by the following formula:

$$\begin{cases} S(\nu) = \dfrac{S(\nu_0)}{\left(1 + \left(\dfrac{|\nu-\nu_0|}{\Delta\nu_S}\right)^b\right)^c} \\ \Delta\nu_S = \Delta\nu_N \, n'^{2.3} \\ b = 0.5\, n' \\ c = \dfrac{5}{2b} \end{cases} \tag{6}$$

Among the four parameters appearing here: $S(\nu_0)$, $\Delta\nu_S$, $b$ and $c$, only two ($\Delta\nu_S$ and $b$) are adjusted independently to fit the theoretical profiles.

Our choice of this parametrization is motivated by four considerations:

i) Choice of an appropriate frequency unit. We have introduced the particular value

$$\Delta\nu_N = \frac{e\, a_0\, F_N}{h\, Z}, \tag{7}$$

which corresponds to a classical Stark shift due to the mean electric field $F_N$ of the surrounding electrons ($a_0$ is the Bohr radius), the "normal" field $F_N$ being defined as

$$F_N = e\left(\frac{4}{3}\pi N_e\right)^{2/3}. \tag{8}$$

We obtain numerically, in cgs units,

$$\Delta\nu_N = 0.48\, N_e^{2/3}/Z. \tag{9}$$

Using the ratio $|\nu-\nu_0|/\Delta\nu_N$ allows one to parametrize the profile without any explicit dependence on the electronic density (plasma conditions enter only through $\Delta\nu_N$). Such a scaling was already introduced by Stehlé (1996). In the particular case of hydrogen lines, it can be verified that the formula given by Clausset et al. (1994) included a factor where the fitted exponent of $N_e$ is 0.688 and 0.690, therefore very close to the exponent 2/3 of $\Delta\nu_N$.

ii) $S(\nu)$ must correctly reproduce the width of the line profile. The parameter $\Delta\nu_S$ is caracteristic of this width and a simple fit to the theoretical profiles leads to a value of $\Delta\nu_S/\Delta\nu_N$ depending mainly on the upper level $n'$ of the transition, as given in Eq. (6).

Independently, Clausset et al. (1994) have obtained similar values (2.257 and 2.377) of the $n'$ exponent to fit the Lyman and Balmer lines of hydrogen. This exponent value of about 2.3 for $n'$ has a reasonnable physical meaning considering that the linear Stark effect on the state $n'$ of a one-electron atom produces a mean energy splitting of the level proportional to $n'^2$ (Griem 1974).

The exponent $b$ gives the shape of the profile $S(\nu)$ in the limited intermediate range where $|\nu-\nu_0|$ is of the same order as $\Delta\nu_S$ (see Fig. 3). The fits to a number of different theoretical profiles give values of $b$ ranging from about 1 to 6. The approximate estimate $b = 0.5\, n'$ can be adopted to account for the general trend. However the parameter $b$ was undefined for a number of profiles that show a central dip, which is obtained when the unshifted Stark components are missing (for example the transitions $1 \longrightarrow 3$ or $2 \longrightarrow 4$). We did not attempt to reproduce correctly the line core in these cases.

iii) $S(\nu)$ must correctly reproduce the far wings of the line profile. The expected asymptotic Holstmark behaviour of the line profile in the far wings is $S(\nu) \sim |\nu-\nu_0|^{-5/2}$ (Griem 1974). The exponent $c$ is then fixed by $bc = 5/2$.

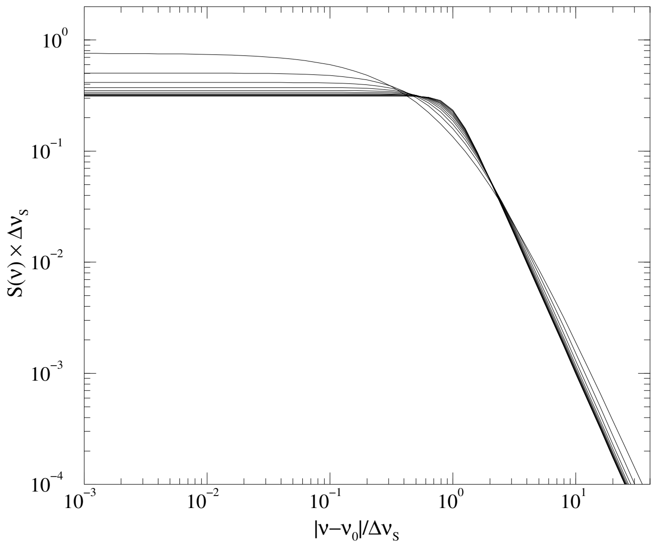


**Fig. 3.** Effect of $b$ on the parametrized profile. In the line core, the value of $S(\nu)$ decreases as $b$ increases from 1 to 6 with a step of 0.5.

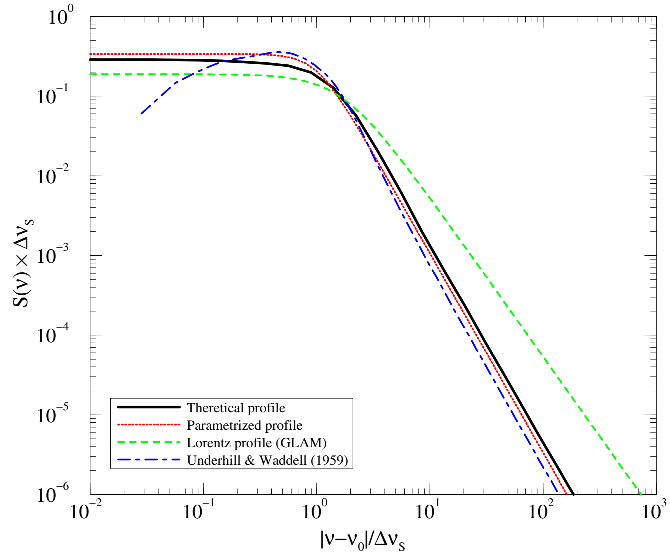


**Fig. 4.** Comparison of our theoretical profile, our parametrized profile, the Lorentz profile used in GLAM, and the profile of Underhill & Waddell (1959) for line 2 → 7 of $C^{5+}$, in the plasma conditions of case 1.

iv) $S(\nu)$ must be normalized to unity. The last parameter $S(\nu_0)$ is then determined by this requirement and can be expressed in terms of the following integral:

$$\Omega_{b,c} \equiv \int_{-\infty}^{\infty} \frac{dx}{\left(|x|^b + 1\right)^c} = \frac{2}{b}\,\frac{\Gamma(\frac{1}{b})\,\Gamma(c - \frac{1}{b})}{\Gamma(c)}, \tag{10}$$

for $b > 0$, $c > 0$, and $bc > 1$, and where $\Gamma$ is the Euler gamma function (see e.g. Gradshteyn & Ryzhik 1994). A simple calculation gives

$$S(\nu_0) = \frac{1}{\Delta\nu_{\rm S}\,\Omega_{b,c}}. \tag{11}$$

For practical purposes, a simple fit of $\Omega_{b,\frac{5}{2b}}$ for values of $b > 1$ can be used, which yields

$$S(\nu_0) \simeq \left(0.3 + \frac{0.46}{b^2}\right) \times \frac{1}{\Delta\nu_{\rm S}}. \tag{12}$$

## 4. Comparison with previous approximations

Before the recent detailed calculations (Stehlé 1994a,b, 1996), astrophysicists have generally introduced linear Stark effect on H-like ions by using the hydrogen available data, the profiles being scaled according to the nucleus charge $Z$. The tables currently used are those of Underhill & Waddell (1959) and those of Vidal et al. (1973).

To perform extensive calculations of stellar opacities and radiative accelerations an analytical form is wanted. A simple procedure introduced by Cox (1965) and adopted by subsequent works (Michaud et al. 1976, GLAM) consisted in keeping Lorentz profiles as for the quadratic Stark effect, but using a Stark width proportional to $n'^5$, instead of the power $n'^4$ given by the usual semi-empirical formula. This artificially broadens the profiles as expected for linear Stark effect, compared with the quadratic case, but the dependance in $n'^5$ is not correct.

An example of profile obtained by the present parametrization is displayed in Fig. 4 for one $C^{5+}$ line (transition 2 → 7). For comparison the graph shows the corresponding original theoretical results (Stehlé 1994a, 1996). It also shows the profile of the same line as derived from the tables of Underhill & Waddell (1959) and the Lorentz function which was previously used as approximation (e.g. GLAM). It appears that the parametrized profile insures a reasonable agreement with the theoretical one from the center to the wings. The data of Underhill & Waddell (1959) show an unreal dip in the line center and because they neglect the electron contribution in the wings, their profile is smaller in the wings by a factor of two. The Lorentz profile cannot reproduce the line wings, even if its width is correctly adjusted in this case.

## 5. The Doppler effect and convoluted profiles

Assuming LTE, the absorbers velocity distribution is Maxwellian and the superposition of the Doppler-shifted line profiles is a convolution of the Stark profile $S(\nu)$ by a Gauss profile of width

$$\Delta\nu_{\rm D} = \frac{\nu_0}{c}\sqrt{\frac{2kT}{m}}. \tag{13}$$

Similarly to the definition of the Voigt function, we define

$$\mathscr{H}_{b,c}(a,v) = \frac{a^{bc-1}}{\sqrt{\pi}\,\Omega_{b,c}} \int_{-\infty}^{\infty} \frac{e^{-y^2}\,dy}{\left(|v-y|^b + a^b\right)^c}, \tag{14}$$

where

$$a = \frac{\Delta\nu_{\rm S}}{\Delta\nu_{\rm D}} \quad \text{and} \quad v = \frac{\nu-\nu_0}{\Delta\nu_{\rm D}}. \tag{15}$$

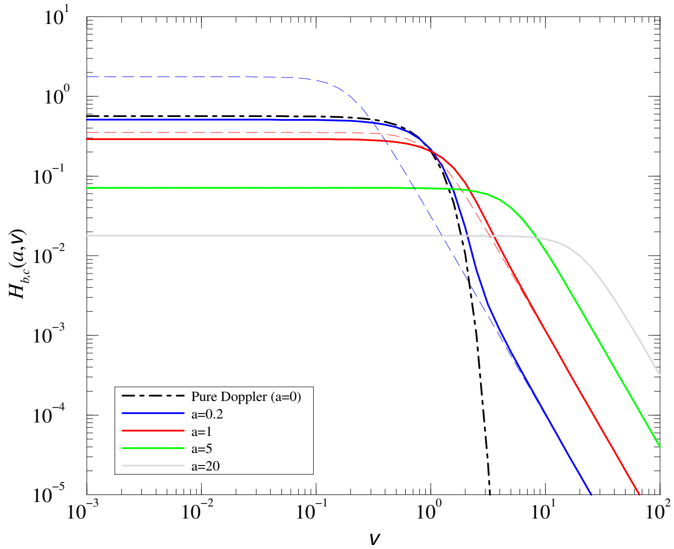


**Fig. 5.** Examples of convoluted profiles $\mathscr{H}_{3,\frac{5}{6}}(a, v)$, for $a$ = 0.2, 1, 5, and 20 (thick solid lines, from left to right in the wings). For comparison, the corresponding parametrized Stark profiles $S$ are also shown (thin dashed lines), along with a pure Doppler profile (thick dot-dashed line).

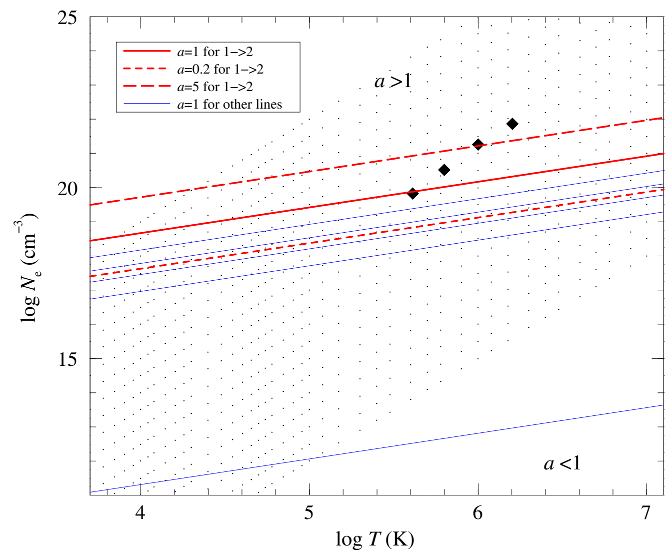


**Fig. 6.** Regions of dominant Doppler or Stark effect for some transitions of $C^{5+}$. The thick lines show, for transition $1 \longrightarrow 2$, the $a$ = 1 line (solid), the $a$ = 0.2 line (short-dashed), and the $a$ = 5 line (long-dashed). The thin lines display, from top to bottom, the $a$ = 1 lines for transitions $1 \longrightarrow 3$, $1 \longrightarrow 4$, $1 \longrightarrow 5$, $2 \longrightarrow 3$, and $13 \longrightarrow 14$.

The function $\mathscr{H}_{b,c}(a, v)$ is normalized in $v$. The relation with the Voigt function is

$$H(a, v) = \sqrt{\pi}\,\mathscr{H}_{2,1}(a, v) \tag{16}$$

(note that $\Omega_{2,1} = \pi$).

The normalized line profile in $\nu$ is then given by:

$$\phi(\nu) = \frac{1}{\Delta\nu_{\rm D}}\mathscr{H}_{b,c}(a, v). \tag{17}$$

Fig. 5 shows examples of some convoluted profiles for several values of $a$, the ratio of Stark width to Doppler width, as well as a pure Doppler profile, for $b = 3$ and $c = \frac{5}{6}$. The corresponding Stark profiles (with the same values of $b$ and $c$) are also shown, the only influence of varying $a$ on the latter is to change the line width and the normalization when using the variable $v$. It can be clearly seen that for values of $a < 1$, the line core is dominated by the Doppler profile, whereas in the far line wings, the Stark component is the most important one. On the other hand, for larger values of $a$, the Stark component dominates the whole profile, and is even indistinguishable from the convoluted profile for $a \geq 5$.

Regions of the $(\log T, \log N_{\rm e})$ diagram where Doppler or Stark contributions dominate are indicated in Fig. 6 for some lines of $C^{5+}$. The "contour lines" for a given value of $a$ (straight lines in this case) are obtained by the equation:

$$\log N_{\rm e}({\rm cm}^{-3}) = \frac{3}{4}\log T({\rm K}) + \frac{3}{2}\log\left(\frac{n'^2 - n^2}{n^2 n'^{4.3}}\right) + \frac{15}{4}\log Z + \frac{3}{2}\log a + 13.98. \tag{18}$$

In the plasma conditions of interest to us, most line profiles shown in Fig. 6 are dominated by the Stark broadening. This is also true for other transitions, as the $a$ = 1 line is lower and lower on the graph as $n$ and $n'$ increase. For nitrogen, and oxygen, the same pattern is observed with a slight vertical shift. For direct comparison, the $a$ = 1 line for transition $1 \longrightarrow 3$ of $O^{7+}$ falls almost exactly on the one for transition $1 \longrightarrow 2$ of $C^{5+}$.

It can also be noticed that $a$ will be larger than 5 for a large number of transitions in cases 1 to 4, the convolution will therefore not be necessary for them.

## 6. Application to the calculation of radiative accelerations

As an example of astrophysical application, we show how the radiative acceleration $g_{\rm rad}$ on carbon is sensitive to the line broadening of the H-like ion $C^{5+}$ in the deep layers of a stellar envelope. The reference values of $g_{\rm rad}$ are those of GLAM, computed for a model with $T_{\rm eff}$ = 8 000 K and $\log g$ = 4.2. Fig. 7 shows the effects of the new profiles which have been introduced by means of the parametrization of Sect. 3 in the same calculation procedure as in GLAM. The atomic data were also taken from TOPbase (Cunto et al. 1993a,b), the atomic database of the Opacity Project (Seaton 1987, 1993). As mentioned earlier, the parametrization is based on theoretical profiles of Balmer and Lyman series for 4 plasma conditions. Because of the regular behaviour of the fitting parameters $\Delta\nu_{\rm s}$ and $b$, we have decided to use the parametrized profiles for all lines (not only for Balmer and Lyman series) and for all plasma conditions where the H-like ions dominate.

Since the new profiles are narrower than those used in GLAM (see Fig. 4), the saturation increases and the predicted

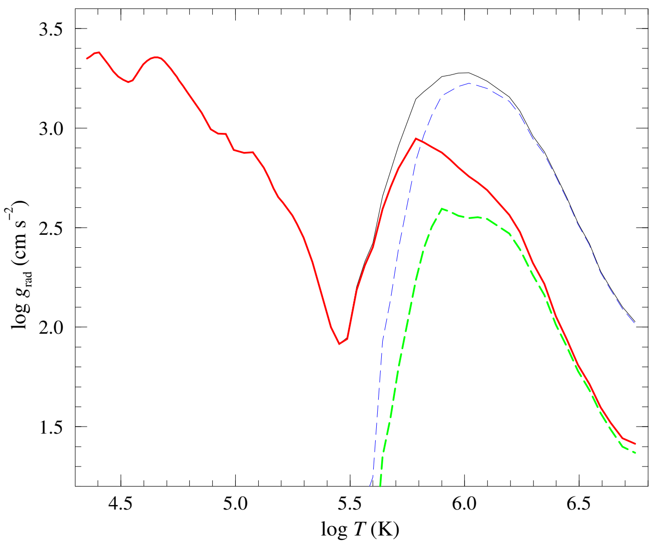


**Fig. 7.** Radiative acceleration on carbon due to b-b transitions, under the convection zone of the model with $T_{eff}$ = 8 000 K and log $g$ = 4.2. The dashed lines show the contribution of the H-like ion $C^{5+}$ and the solid lines show the sum of the contributions of all carbon ions. Previous calculations (GLAM) are displayed with thin lines, while our new results are presented with thick lines.

values of $g_{rad}$ are smaller. For about log $T$ = 5.9, the radiative acceleration, which is dominated by the $C^{5+}$ contribution, is decreased by a factor of 4.5 compared to the previous result of GLAM. This amplifies the trend of carbon to sink inside stellar envelopes.

However, this calculation included the b-b transitions only. The contribution of b-f transitions was also computed in GLAM, using photoionization cross-sections from TOPbase, and appeared to be significant at higher temperatures, for log $T \gtrsim 5.6$. Uncertainty on the $f_{ion}$ factor (see Sect. 6 of GLAM) affects the predicted b-f contribution. We obtained preliminary results using a better approximation for $f_{ion}$ (Massacrier 1996) which show that the b-f contribution to $g_{rad}$ does not change significantly. A detailed study of the b-f and f-f contributions to the radiative acceleration on H-like and He-like ions will be given in a subsequent paper.

## 7. Conclusion

This paper is a follow-up to a previous work (GLAM) achieving a detailed calculation of radiative accelerations in stellar envelopes. The extensive use of the recently available atomic databases allowed to compute the spectrum of the background opacity with a good frequency resolution. Concerning the line profiles which have an important effect on saturation, the quadratic Stark broadening was evaluated in GLAM by means of a semi-empirical method. The linear Stark effect, which is dominant for one-electron ions, was not yet taken into account. The purpose of the present paper is to include more realistic lines profiles for H-like ions, especially for elements C, N, and O which are major absorbers in stellar plasma.

We have computed theoretical Stark profiles of the Lyman and Balmer series of the H-like ions $C^{5+}$, $N^{6+}$, and $O^{7+}$ for a range of stellar plasma conditions where they represent more than 50% of their species. They have been summarized in a convenient analytical formula, whose parameters depend only on the electronic density (through $\Delta\nu_N$) and on the principal quantum number $n'$ of the upper level of the transition. Comparisons with the theoretical profiles as well as with other approximations show that this formula gives a reasonable accuracy in view of astrophysical applications. It can also be used for series other than Lyman and Balmer.

Thanks to the simple analytical formulae fitting these profiles, it will become easy to improve the calculation of detailed monochromatic opacities, as required in a number of astrophysical modelizations. Due to the wavelength coincidences occurring between H-like spectra, the knowledge of an accurate profile is particularly critical to predict saturation effects.

An example of their influence on radiative acceleration is given. The contribution of b-b transitions to $g_{rad}$ in the regions where the H-like ion is dominant is found to be significantly reduced compared to previous work. The total radiative acceleration will therefore be more sensitive to the contribution of the b-f and f-f transitions. This latter problem will be addressed in a subsequent paper.

Richer et al. (1998) have recently developed stellar evolution models taking simultaneously into account atomic diffusion and its effects on the stellar structure through the Rosseland mean opacity. Their application to the sun (Turcotte et al. 1997) and to F and A-type stars (Turcotte 1997) shows that the variations of $g_{rad}$ through the entire envelope can affect the surface abundances. Additionaly, C, N, and O are so large contributors to the Rosseland opacity that the stellar structure is sensitive to local variations of their abundances, even in deep layers of the envelope. The contributions of H-like ions to the radiative acceleration must therefore be evaluated accurately, and the line profiles given here should be included in future calculations.

## References

Baranger, M., Mozer, B., 1959, Phys. Rev. 115, 521
Baranger, M., Mozer, B., 1960, Phys. Rev. 118, 626
Brissaud, A., Frisch, U., 1971, JQSRT 11, 1767
Clausset F., Stehlé, C., Artru, M.-C., 1994, A&A 287, 666
Cox, A.N., 1965, Stellar structure. In: Aller, L.H., McLaughlin, D.B. (eds) Stars and Stellar Systems, Vol. 8, University of Chicago, Chicago Press, p. 218
Cunto, W., Mendoza, C., Ochsenbein, F., Zeippen, C.J., 1993a, Bull. Inf. CDS 42, 39
Cunto, W., Mendoza, C., Ochsenbein, F., Zeippen, C.J., 1993a, A&A 275, L
Demura A.V., Gilles, D., Stehlé, C., 1995, JQSRT 54, 123
Eissner, W., Jones, M., Nussbaumer, H., 1974, Comput. Phys. Commun. 8, 270
Gonzalez, J.-F., Artru, M.-C., Michaud, G., 1995a, A&A 302, 788

Gonzalez, J.-F., LeBlanc, F., Artru, M.-C., Michaud, G., 1995b, A&A 297, 223
Gradshteyn, I.S., Ryshik, I.M., 1994, Table of Integrals, Series and Products, Academic Press, 5th ed.
Greene, R.L., Cooper, J., 1975, JQSRT 15, 1037
Griem, H.R., 1974, Spectral Line Broadening by Plasmas. Academic Press, Nwe York
Massacrier, G., 1996, A&A 309, 979
Michaud, G., Charland, Y., Vauclair, S., Vauclair, G., 1976, ApJ 210, 447
Richer, J., Michaud, G., Rogers, F.J., et al., 1998, ApJ, in press
Schönig, T., 1994, A&A 282, 994
Schönig, T., Butler, K., 1989, A&AS 78, 51
Seaton, M.J., 1987, J. Phys. B 20, 6363
Seaton, M.J., 1993, In: Weiss, W.W., Baglin, A. (eds.) Proc. IAU Coll. 137, Inside the stars. PASPC, Vol. 40, p. 246
Stehlé, C., 1994a, A&AS 104, 509
Stehlé, C., 1994b, A&A 292, 699
Stehlé, C., 1996, A&A 305, 677
Turcotte, S., Ph.D.thesis, Université de Montréal
Turcotte, S., Richer, J., Michaud, G., Iglesias, C.A., Rogers, F.J., 1997, ApJ, submitted
Underhill, A.B., Waddell, J.H., 1959, National Bureau of Standards Circular 603
Vidal, C.R., Cooper, J., Smith, E.W., 1973, ApJS 25, 37

This article was processed by the author using Springer-Verlag LaTeX A&A style file *L-AA* version 3.